The Journal of Experimental Biology 202, 757–770 (1999)
Printed in Great Britain © The Company of Biologists Limited 1999
JEB1854

HOW POLARIZATION-SENSITIVE INTERNEURONES OF CRICKETS SEE THE POLARIZATION PATTERN OF THE SKY: A FIELD STUDY WITH AN OPTO-ELECTRONIC MODEL NEURONE

T. LABHART*

Zoologisches Institut der Universität, Winterthurerstrasse 190, CH-8057 Zürich, Switzerland

*e-mail: labhart@zool.unizh.ch

Accepted 13 January; published on WWW 9 March 1999

Summary

Many insects gain directional information from the polarization pattern of the sky. Polarization vision is mediated by the specialized ommatidia of the dorsal rim area of the compound eye, which contains highly polarization-sensitive photoreceptors. In crickets *Gryllus campestris*, polarized light information conveyed by the dorsal rim ommatidia was found to be processed by polarization-opponent interneurones (POL-neurones). In this study, a field-proof opto-electronic model of a POL-neurone was constructed that implements the physiological properties of cricket POL-neurones as measured by previous electrophysiological experiments in the laboratory. Using this model neurone, both the strength of the celestial polarization signal and the directional information available to POL-neurones were assessed under a variety of meteorological conditions. We show that the polarization signal as experienced by cricket POL-neurones is very robust, both because of the special filtering properties of these neurones (polarization-antagonism, spatial low-pass, monochromacy) and because of the relatively stable e-vector pattern of the sky.

Key words: polarization vision, interneurone, model neurone, filter, cricket, *Gryllus campestris*, vision.

Introduction

Skylight polarization offers insects a useful reference in visual compass orientation for navigation or cruising-course control. The cricket (*Gryllus* sp.) is one of the insects in which polarization vision has been studied most thoroughly (e.g. Burghause, 1979; Labhart et al., 1984; Brunner and Labhart, 1987; Nilsson et al., 1987; Labhart, 1988, 1996; Herzmann and Labhart, 1989; Zufall et al., 1989; for a review, see Labhart and Petzold, 1993). As in other insects (for a review, see Labhart et al., 1992), polarization vision in crickets is mediated by a comparatively small group of specialized ommatidia situated at the dorsal rim of the compound eye. Only in crickets and locusts, and recently also in the desert ant *Cataglyphis bicolor*, has the processing of polarized light information by the insect visual system been studied successfully beyond the level of the retina by recording from polarization-sensitive interneurones in the optic lobe (crickets: Labhart, 1988, 1996; Labhart and Petzold, 1993; Petzold and Labhart, 1993; Helbling and Labhart, 1997; Petzold, 1999; locusts: Homberg and Würden, 1997; ants: T. Labhart, unpublished observations) and in the central complex of the brain (locusts: Müller and Homberg, 1994; Müller, 1997; Vitzthum, 1997; Vitzthum et al., 1997). The so-called POL-neurones of field crickets *Gryllus campestris* receive input from the highly polarization-sensitive blue-receptors of the dorsal rim area of the eye. In these neurones, spike activity is a sinusoidal function of e-vector orientation with an excitatory and an inhibitory part, and with the maxima and minima separated by 90°. Thus, POL-neurones are polarization-opponent neurones receiving antagonistic input from two analyzer channels with orthogonal orientations of maximal sensitivity (Labhart, 1988). The two analyzer channels are represented by two sets of photoreceptors with orthogonally arranged microvilli, present in each dorsal rim ommatidium (Burghause, 1979). Each POL-neurone receives antagonistic input from a large number of dorsal rim ommatidia (Helbling and Labhart, 1997; T. Labhart unpublished observations). The polarization-antagonism makes the e-vector response of POL-neurones intensity-independent and enhances sensitivity for e-vector contrasts (Labhart, 1988; Labhart and Petzold, 1993). The POL-neurones are colour-blind since the dorsal rim area is monochromatic, containing only blue-receptors (Labhart et al., 1984; Zufall et al., 1989; Labhart, 1988), and within their wide visual fields the POL-neurones are indifferent to the position of a polarized stimulus (Labhart and Petzold, 1993; Petzold, 1999). However, the POL-neurones are strongly sensitive to the orientation of the e-vector of polarized light even when the polarization signal is very weak (Herzmann and Labhart, 1989; Labhart, 1996).

Previous studies on POL-neurones were performed under rather artificial stimulus conditions. Compared with the sky,

either the angular extent of the stimulus was very small (1–2 °) or the degree of polarization was unnaturally high (or both). Although such experiments are perfectly suitable for characterizing the physiological properties of POL-neurones, they are not suited to assess the response to the natural stimulus, the polarization pattern of the sky. The straightforward approach, i.e. to perform the recordings in the field, is ruled out by the difficulty of recording from POL-neurones, even under laboratory conditions. Therefore, a field-proof model POL-neurone in the form of an opto-electronic device was constructed on the basis of the physiological properties of cricket POL-neurones measured in the laboratory experiments. Using this model, both the strength of the celestial polarization signal and the directional information available to a POL-neurone can be assessed under a variety of meteorological conditions. In other words, using this model, the sky can be viewed as seen by an insect eye. In this study, we show that the polarization signal in the sky as experienced by a POL-neurone is very robust, both because of the filtering properties of the neurone and as a result of the relatively stable e-vector pattern of the sky.

Materials and methods

The opto-electronic model POL-neurone

(A) Photoreceptors

Opto-electronic representations of insect photoreceptors were built using photodiodes fitted with blue filters, the signals of which were logarithmized. More specifically, we used ultraviolet-enhanced silicon photodiodes with built-in JFET linear operational amplifiers (UDT-O55UV; Photops series of United Detector Techology) with a circular active surface 8 mm in diameter. The amplifiers delivered a voltage that was proportional to the photon flux, and their gain was adjusted to the current level of light intensity. The wideband blue filters (BG 28, 2 mm thick, Schott) in combination with the photodiodes provided maximal sensitivity at approximately 450 nm with a 130 nm bandwidth, corresponding approximately to the spectral sensitivity of the blue-receptors in the dorsal rim area of the cricket (Labhart et al., 1984). The signals were then logarithmized by logarithmic amplifiers (SSM-2100, Precision Monolithic Inc., or LOG100, Burr Brown) adopting the approximately logarithmic intensity characteristic of insect photoreceptors (e.g. Laughlin, 1981). Three photodiodes were mounted on the outside of a metal box, which contained some of the electronics. To restrict the visual field, they were surrounded by metal cylinders lined with black antireflective coating (41 mm inner diameter). Visual field size was adjusted by using different lengths of cylinders (Figs 1A, 2A). Adopting the approximate visual field size of cricket POL-neurones (Petzold, 1999), the aperture was 60 ° and was centred at 25 ° from the zenith. To test the influence of visual field size, smaller and larger apertures were used in some experiments (see Results). Exact centring of the photodiodes within the parallel cylinders provided identical receptive fields for all three photoreceptors at infinity. The absolute sensitivity of the three photoreceptors was exactly matched such that equal photon fluxes produced equal voltage signals at the output. Two of the photoreceptors were equipped with polarizers (HNP'B, Polaroid Company) mounted on top of the cylinders. In one of these, the e-vector transmission axis was exactly horizontal; in the other, the axis was vertical (horizontal and vertical polarization channels). The third receptor was fitted with a neutral density filter with approximately the same transmission as the polarizers (intensity channel) (Figs 1A, 2A).

(B) Polarization-opponent mechanism

The polarization-antagonism found in cricket POL-neurones was implemented by subtracting the logarithmized signal of the two polarization channels from one another, with the horizontal channel defined as positive. In a first version of the model with the SSM-2100 as logarithmizer, the signals were subtracted from one another by a differential amplifier. In the final version, with which most experiments were performed, the LOG100 chip both logarithmized and subtracted the signals. The output signal V_{out} of the model POL-neurone is thus given by:

$$V_{out} = \log V_{hor} - \log V_{vert} = \log(V_{hot}/V_{vert}), \quad (1)$$

where V_{hor} and V_{vert} are the outputs of the first-stage photodiode amplifiers of the polarization channels.

Scanning mechanism

The model POL-neurone was mounted on a vertical axle driven by a direct-current motor with a strongly reducing gear, providing a constant angular velocity of 15 ° s^{-1} (Figs 1A, 2A). An incremental angle encoder (G38, Litton Servo Technik) provided trigger and calibration signals for azimuthal orientation.

Data recording

Data were recorded with a four-channel digital recorder equipped with a memory card (model 8830, Hioki Corporation) providing eight-bit sampling depth and an angular resolution of approximately 0.15 ° (approximately 2450 sample points in 24 s). The following data were recorded: (1) the signal of the model POL-neurone (see above), (2) the logarithmized signal of the intensity sensor, (3) two trigger pulses indicating the beginning (0 °) and completion (360 °) of the scan, and (4) calibration pulses every 10 ° to check for possible variations in angular velocity during a scan.

Experimental procedures

For the measurements, the roll-cart with the equipment was moved to the flat roof of the university building. The scanner was levelled, and its azimuthal orientation was adjusted using a distant landmark such that each scan started exactly South with the rotation axis pointing to the zenith. To avoid overloading the photodiodes by direct sunlight at high solar elevations, a circular screen of diameter 40 cm placed at 3–4 m distance shaded the scanner (the angular size of the shade was

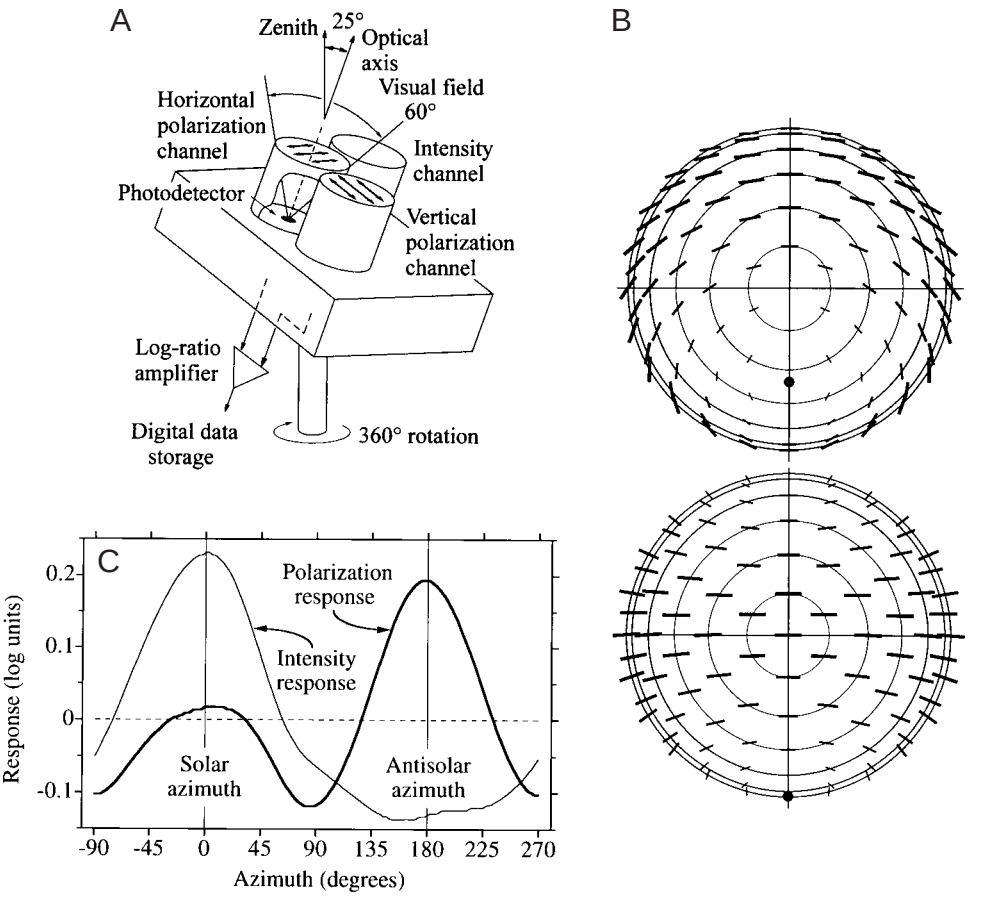

Fig. 1. (A) Schematic drawing of the opto-electronic model of a polarization-opponent neurone (POL-neurone). (B) Polarization pattern of the sky (two-dimensional plot) for two elevations of the sun (filled circle; top 55 °, bottom 5 °). Concentric circles indicate parallels of latitude of the celestial hemisphere with the zenith at the centre. e-vector orientations (indicated by the bars) are plotted with respect to the tangent to the parallel of latitude at the positions indicated (compare Fig. 2a in Schwind and Horváth, 1993). In this representation of the polarization pattern, e-vectors can be read directly from the graph; specifically, e-vectors that are parallel in the sky also appear parallel in the graph. The degree of polarization *d* is indicated by the length and width of the bars. (C) Typical response curve of the POL-neurone model obtained under a cloudy sky (compare Fig. 2B). The maxima of the polarization signal (thick line) are indicators of the solar (0 °) and the antisolar (180 °) azimuth. The intensity signal (thin line) shows that there is a steep intensity gradient in the sky. The ordinate indicates the model response in logarithmic units (dimensionless; see text).

maximally about 10 ° or 3 % of the visual field size). Just before triggering a 360 ° scan, the shade was carefully adjusted and the time was recorded to the minute. To record the actual sky condition during each scan, a colour photograph of the sky was taken with a 180 ° fisheye lens centred on the zenith.

Evaluation of data

The digitized data were transferred to a Macintosh computer and evaluated using a program written in IGOR Pro 2.04 (WaveMetrics Inc.). To remove high-frequency noise that might interfere with the evaluation process, intensity and polarization signals were slightly smoothed using a 21-point window (corresponding to approximately 3 °). This process did not influence the general shape of the response curves. The voltage response V_{out} of the model was converted such that the response curve expressed the logarithm of the relative activations of the two polarization channels, i.e. $R=\log(V_{hor}/V_{vert})$. No significant variations in angular velocity were observed during a scan so that time (0–24 s) could be linearly converted to azimuth (0–360 °).

The recorded response curves of the model neurone are characterized by two maxima (and two minima) near the solar and the antisolar azimuth, respectively (see Figs 1C, 3A,B). The strength of the polarization signal in the sky, termed the effective degree of polarization d_{eff}, was calculated in the following way for both the solar and the antisolar half of the sky. First, the program determined the modulation amplitude *M* of the response:

$$M = R_{max} - \overline{R_{min}}, \quad (2)$$

where R_{max} is the highest value of the response maximum and $\overline{R_{min}}$ is the average of the lowest response levels of the two minima. Second, the linearized response amplitude $P=10^{M/2}$ for one polarization-sensitive channel was calculated, the exponent being *M*/2 (and not *M*) to remove the effect of the polarization antagonism on the amplitude. Thus, *P* expresses the ratio of the maximal (V_{max}) and the minimal (V_{min}) responses to the e-vector (i.e. excluding any effects of an intensity gradient in the sky) of either the horizontal or the vertical polarization channel when the model neurone scans the sky with its eccentric visual field; thus, $P=V_{max}/V_{min}$. Finally, the program calculated the effective degree of polarization d_{eff} as:

$$d_{eff} = (P - 1)/(P + 1). \quad (3)$$

The definition of d_{eff} requires some explanation. The degree of polarization *d* of a light source is usually defined as:

$$d = \frac{V_{max} - V_{min}}{V_{max} + V_{min}} = \frac{(V_{max}/V_{min}) - 1}{(V_{max}/V_{min}) + 1}, \quad (4)$$

where V_{max} and V_{min} are the maximum and minimum responses, respectively, obtained when a polarized light source is viewed by a linear photodetector through a polarizer whose

preferred plane is rotated. Substituting V_{max}/V_{min} in the equation with P, one obtains the definition of d_{eff} given in equation 3, indicating that d_{eff} follows the usual definition of d.

For the local degree of polarization d_{loc} within the 60 ° visual field at the solar and the antisolar azimuth, P can be directly calculated from R_{max}. This is because the celestial e-vector orientation is horizontal in these directions and, therefore, R_{max} indicates the response ratio of the two analyser channels. Thus:

$$P_{loc} = 10^{R_{max}} \quad (5)$$

and

$$d_{loc} = (P_{loc} - 1)/(P_{loc} + 1)\,. \quad (6)$$

The azimuth of the response maxima was assessed using two methods. (1) The median method. First, the 'maximum range' of a response curve was selected, defined by a 45 ° window such that the left and right borders of the window were at the same response level. The position of the maximum Az_{med} was defined by that azimuth for which the areas under the curve to the left and right of Az_{med} were equal. (2) The maximum-value method. To avoid the influence of residual noise, the response curve was first smoothed by a 51-point window (approximately 7.5 °). The position of the maximum Az_{max} was then defined by the azimuth showing the highest response value.

For most measurements, the solar elevation and the solar azimuth for each experiment were determined by an astronomical computer program (The Earth Centered Universe, Nova Astronomics) with a maximal error of approximately ±0.15 ° (corresponding to 1 min time resolution). For the first measurements, an astronomical table was used for this purpose with a slightly larger errror. The azimuth error of the model POL-neurone was defined by the difference between the actual solar or antisolar azimuth and the azimuth of the respective maximum (Az_{med} or Az_{max}) indicated by the response function. Positive error values indicate counterclockwise deviations as seen when looking up to the sky. To compare the performance of the model neurone under different conditions, error distributions (unsigned error values) were tested against each other using the Mann–Whitney U-test.

Results

Measurements were made on 19 days during two autumn seasons (mid September to early November) under a wide variety of sky conditions ranging from clear and cloudless skies to totally overcast skies and with solar elevations ranging from 0 to 44 °. Using the fisheye photographs, the condition of the upper part of the sky (above 30 ° elevation) was classified for each experiment, separately for the solar and the antisolar half of the sky. Four classes of sky condition were defined: sky 0, no clouds visible, but some diffuse haze possible; sky 1, clouds covering up to 50 % of the sky; sky 2, more than 50 % clouds, but at least some specks of blue sky visible; sky 3, total, but sometimes thin, overcast, no blue sky visible.

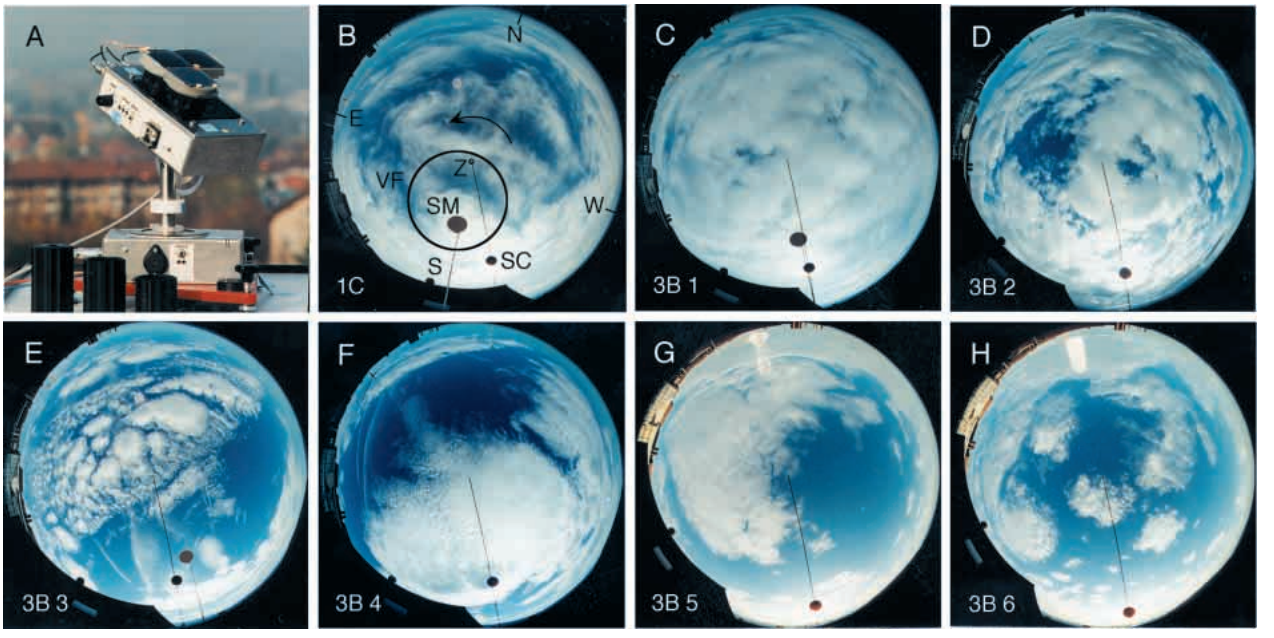

Fig. 2. (A) Photograph of the POL-neurone model (see the schematic drawing in Fig. 1A). Different-sized black tubes shown in the foreground serve to adjust the visual field (normally 60 °). (B–H) 180 ° fisheye photographs of the skies for which the response curves are given in Figs 1C and 3B. The zenith (Z) is at the centre, and the horizon is at the circumference of the photographs. (B) Sky condition for the response curve in Fig. 1C. VF is the outline of the 60 ° visual field of the model; the arrow indicates the sense of 360 ° rotation starting in the South (S). SC is the sun screen for the camera and indicates the position of the sun in the photograph. SM is the sun screen shading the model neurone from direct sunlight. (C–H) The numbers of the corresponding response curves given in Fig. 3B are indicated in the lower left corner of each photograph. In all sky photographs, the symmetry line of the polarization pattern is indicated by the black marker line. Bright areas near the antisolar horizon in G and H are caused by reflections of sunlight in the camera lens at low solar elevations.

During each experiment, the model neurone made a 360° rotation in the counterclockwise direction (as seen when looking up to the sky) starting exactly in the South (see Fig. 2B). Thus, by scanning the sky, a modelled POL-neurone response can be recorded for each azimuthal direction. A typical response curve and the photograph of the actual sky condition are presented in Fig. 1C (polarization response) and Fig. 2B. The response curve exhibits two maxima, one close to the solar azimuth and the other close to the antisolar azimuth; this is because the e-vector tuning angle of the positive analyser channel corresponds with the horizontal e-vector orientation (for details, see Materials and methods). Since the e-vector orientation is horizontal along the whole solar/antisolar meridian (the symmetry line of the polarization pattern; see Fig. 2B), the response maxima must always be expected at the solar and at the antisolar azimuth, irrespective of solar elevation. The antisolar maximum is larger than the solar maximum because the degree of polarization in the antisolar half of the sky is larger than in the solar half. Since the polarization pattern is somewhat disturbed by clouds (Fig. 2B), the maxima are not perfect indicators of the solar and the antisolar azimuth in this example. The model responses presented in Fig. 1C and Fig. 3A–C express the logarithm of the relative activations of the two polarization channels (see Materials and methods). The response curves thus simulate the modulation of the real neural response.

Strength of the polarization signal

The amplitude of the POL-neurone response, and therefore the strength of the polarization signal, depends on different factors in a rather complicated, mutually interacting way. (1) Solar elevation: both the degree of polarization and e-vector alignment within the 60° visual field are functions of angular distance from the sun, reaching a maximum at 90° (see Fig. 1B). The highest maxima are therefore expected in the antisolar direction with low solar elevations. The minima are subject to the same influences. But, in addition, the minima are affected by a mismatch between the vertical tuning angle of the negative channel and the e-vector orientation orthogonal to the solar/antisolar meridian (except for 0° solar elevation) (see Fig. 1B). Thus, the minima will decrease in size with increasing solar elevation. For response curves with different solar elevations under clear skies, see Fig. 3A. (2) Sky condition: both haze and clouds within the visual field of the neurone reduce the degree of polarization and, therefore, the strength of the polarization signal. Response curves obtained under cloudy skies are exemplified in Fig. 3B (curves 1–6), and photographs of the corresponding sky conditions are given in

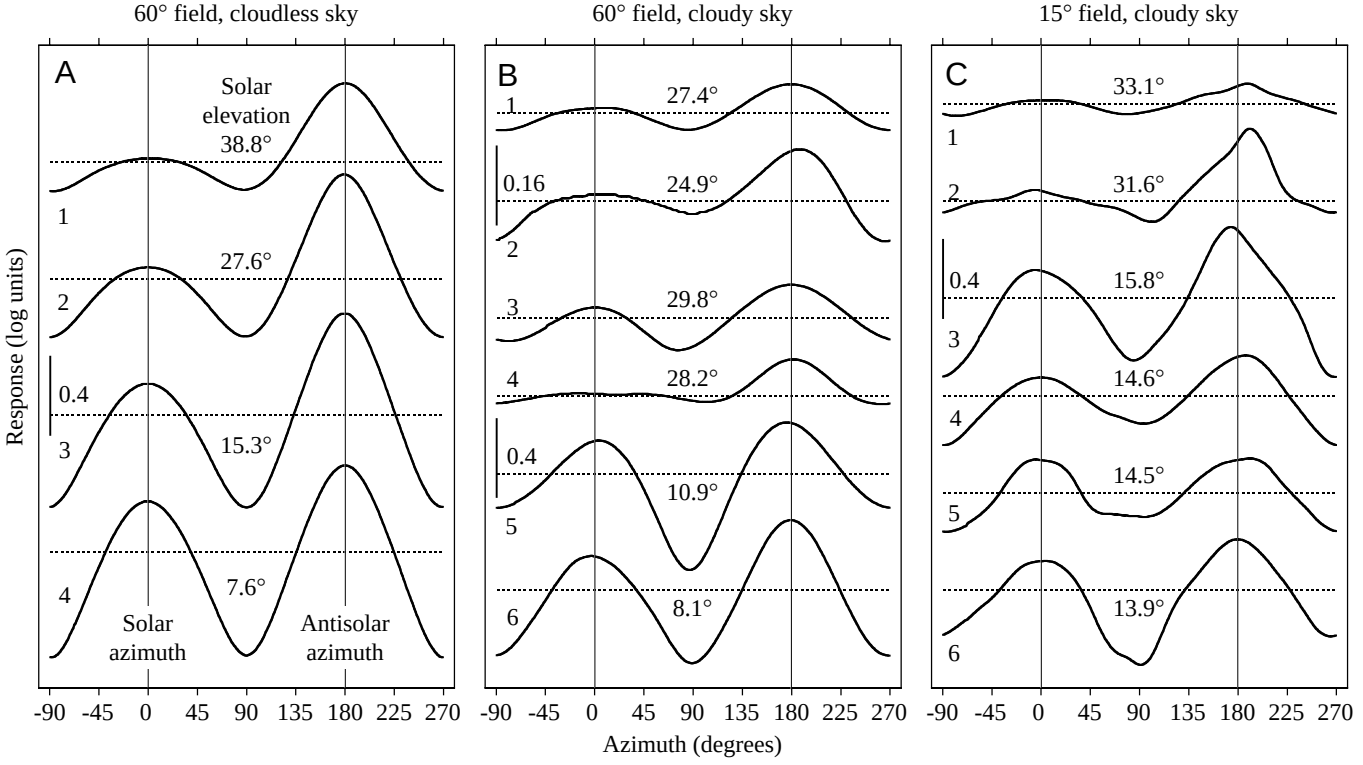

Fig. 3. Examples of response curves of the POL-neurone model (polarization responses). Horizontal dotted lines indicate zero levels of signals (see Fig. 1C). (A) 60° visual field with cloudless skies, (B) 60° visual field with cloudy skies, (C) 15° visual field with cloudy skies. Response calibration is the same for all curves except for the two top curves in B (see calibration bars). Sky conditions for response curves B1–B6 are given in Fig. 2C–H (see numbers in lower left corner of photographs). Note the smooth shape of the response curves and the symmetrical maxima under all sky conditions with the 60° visual field (A,B). In contrast, with 15° visual fields, the curves have irregular shapes and asymmetrical maxima under cloudy skies (C).

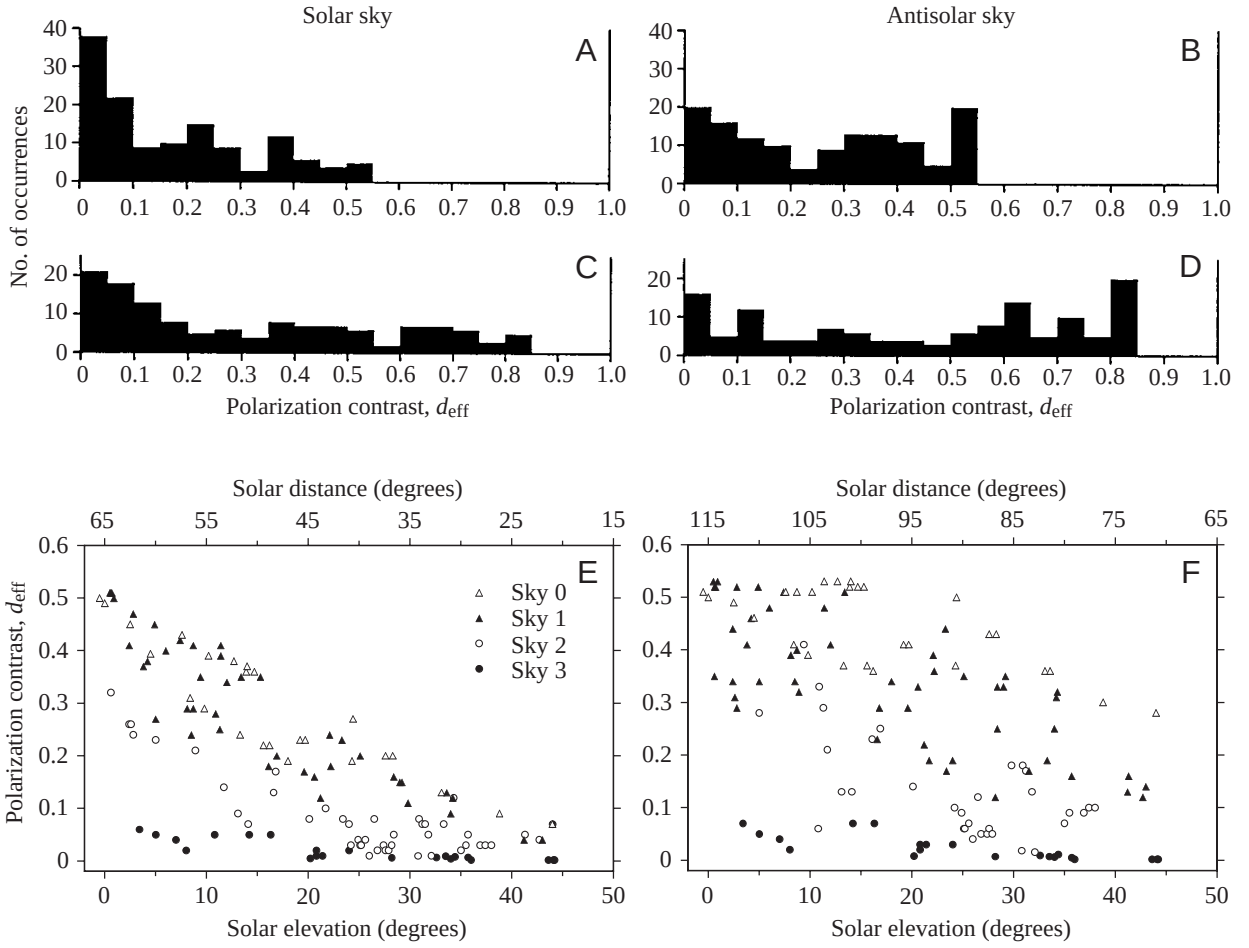

Fig. 4. Polarization contrast d_{eff} in the solar and in the antisolar part of the sky (left and right column, respectively). (A,B) Histograms of polarization contrast d_{eff} in the sky, i.e. as experienced by one polarization channel. (C,D) Histograms of d_{eff} as experienced by the POL-neurone model due to the intrinsic polarization antagonism. (E,F) Polarization contrast d_{eff} in the sky as a function of solar elevation (lower abscissa) and solar distance (upper abscissa). Solar distance is defined as the angle between the sun and the optical axis of the model when directed at the solar (E) or the antisolar (F) azimuth. Different symbols code for sky conditions: sky 0, cloudless; sky 1, ⩽50 % cloud; sky 2, >50 % cloud; sky 3, 100 % cloud. N=133 for all graphs. For the definition of d_{eff}, see the text.

Fig. 2C–H (see curve numbers in the lower left corner of each photograph).

Since no calibration factor is available to convert our response units to membrane potential or spike frequency, the response amplitude is expressed in terms of the polarization contrast to which the model was exposed when scanning the sky. Making use of our previous electrophysiological experiments, this measure can be related to spike frequency modulation in cricket POL-neurones and will be compared with astrophysical data on sky polarization (see Discussion). The polarization contrast was calculated separately for the solar and the antisolar half of the sky from the modulation amplitude of the model, i.e. from the difference between a maximum and the two flanking minima. Because this polarization contrast is, in effect, a degree of polarization, we termed it the effective degree of polarization d_{eff} (for details, see Materials and methods). Correspondingly, the limits of d_{eff} are 0 (no contrast) and 1 (maximal contrast).

The complete record of the d_{eff} values observed during our experiments for both the solar and the antisolar half of the sky is given in Fig. 4A,B. Although the data represent a wide range of different sky conditions, the d_{eff} distributions should not be regarded as typical frequency spectra of d_{eff}. The highest values, in particular, are over-represented because we tried to establish the upper limit of d_{eff} in the clear sky on several occasions. As expected, d_{eff} in the solar sky is generally lower than in the antisolar sky. The maximal value of d_{eff} ever recorded was 0.53. The polarization contrast as experienced by the POL-neurone model internally due to the polarization antagonism is shown in Fig. 4C,D and will be discussed below (see Discussion).

In Fig. 4E,F, the d_{eff} values are plotted with respect to both solar distance (see upper abscissa) and solar elevation (see lower abscissa). Solar distance is defined as the angle between the sun and the optical axis of the model when directed at the solar (Fig. 4E) or the antisolar (Fig. 4F) azimuth. Different symbols code for actual sky condition (sky 0 to sky 3). The d_{eff} values in the solar half of the sky (Fig. 4E) show a stronger

dependence on solar elevation than those in the antisolar sky (Fig. 4F). This is because the solar values cover a celestial range from very close to the sun, where the degree of polarization is very small, to 65° solar distance with rather strong polarization, whereas the gradient of polarization is small within the celestial range of the antisolar values. As expected, the polarization contrast d_{eff} is largest with a low sun in a cloudless (open triangles) or only slightly cloudy (filled triangles) sky. A few light clouds seem to reduce d_{eff} less than does some haze (upper filled triangles *versus* lower open triangles). The smallest polarization contrasts were obtained in the solar sky with high sun and under heavily clouded skies (filled circles).

To test the influence of visual field size on the strength of the polarization signal, some measurements were made with apertures that were smaller (7.5° or 15°) and larger (90°) than usual (60°). For appropriate comparison, the tests were carried out under a cloudless sky and by alternating between different field sizes. The smaller apertures increased the solar d_{eff} by 25% and the antisolar d_{eff} by 15%. The larger aperture reduced the solar d_{eff} by 33% and the antisolar d_{eff} by 23% (Table 1). Thus, d_{eff} decreases with increasing aperture, and this dependence is stronger in the solar part of the sky. On consulting the e-vector pattern of the sky (Fig. 1B, top), it becomes evident that this effect must be a consequence of the variation in e-vector orientation within the visual field.

Directional information of the polarization signal

As explained above, the two maxima of the response curves should indicate the solar and the antisolar azimuths. The deviation of the measured response maximum from the theoretical maximum (error) can therefore be taken as a measure of the precision of directional information conveyed by the model POL-neurone. Maxima with polarization contrast $d_{eff}<0.01$ were excluded from this evaluation because such weak signals, which occurred only under strongly overcast skies, often resulted from spurious response modulations (see also Brines and Gould, 1982).

Fig. 5 shows the observed errors for both the solar (left column of Fig. 5) and the antisolar (right column of Fig. 5) sky. These errors (Err_{med}) were calculated by using the azimuths of the response maxima obtained by the 'median method' (see Materials and methods) (for comparison with azimuths based on the 'maximum-value method', see below). Fig. 5A,B gives the data for all sky conditions (sky 0 to sky 3). In almost all response curves, two clearly defined maxima were present (for examples, see Fig. 3A and Fig. 3B curves 1–3, 5 and 6). In only eight cases was the solar maximum undefined (two small maxima or one very flat maximum; for an example, see Fig. 3B curve 4) and, therefore, no error value could be calculated. In Fig. 5E–M the data are presented separately for the different sky conditions, and these indicate that the best performance (smallest errors) is achieved under cloudless skies, as expected. Note, that the errors remained below 10° in most cases, even under strong cloud cover. Under cloudless skies (sky 0), the errors were always very small (Fig. 5E,F), mostly within ±0.5°. Rather than indicating actual errors of the polarization signal, this value probably reflects the overall error of the measuring system due to limited angular resolution (see Materials and methods) and small calibration errors.

In Fig. 5N,O, the errors are plotted *versus* polarization contrast d_{eff}. Different symbols code for actual sky condition (as in Fig. 4E,F). They show that large errors (>12°) and undefined maxima occurred with strong cloud cover (sky 2 and sky 3) and with very low polarization contrast only. As discussed below (see Discussion), d_{eff} values of less than 0.05 are too low to be physiologically relevant. Fig. 5C,D gives those error values for which the polarization contrast d_{eff} was greater than 0.05 and that were obtained under experimentally interesting, i.e. cloudy, skies (sky 1 to sky 3). In all these cases, the maxima were clearly defined and the largest error was 12°. Most errors were smaller than ±3.0°, i.e. 85% in the solar sky and 75% in the antisolar sky. For $d_{eff}>0.05$, the precision of the polarization signal was quite independent of polarization contrast (see Fig. 5N,O). Large deviations were always correlated with asymmetric clouding. Clear sky on one side of the symmetry line of the polarization pattern and clouds on the other side shifted the maximum to the clearer sky part (compare, for instance, Fig. 3B curve 5 with Fig. 2G, and Fig. 3B curve 2 with Fig. 2D).

Considering the sometimes strong disturbance of the polarization pattern, the precision of directional information given by the maxima of the POL-neurone signal is astonishingly high. In addition, under physiologically relevant polarization conditions ($d_{eff}>0.05$), the response curves were always smooth and the maxima had quite symmetrical shapes (see Fig. 3A,B). An important agent in stabilizing the polarization signal may be optical integration by the large visual fields of POL-neurones evening out local disturbances of skylight polarization. To test this hypothesis, a number of measurements were performed using apertures of 15° or 7.5° along with the usual 60° visual fields. In Fig. 6, the errors

Table 1. *Influence of visual field size on polarization contrast* d_{eff}

	d_{eff} in proportion to d_{eff} with 60° visual field					
	With 7.5° or 15° visual field			With 90° visual field		
Sky part (solar distance)	Mean	Range	*N*	Mean	Range	*N*
Solar (33–53°)	1.25	1.23–1.28	4	0.67	0.65–0.69	2
Antisolar (83–103°)	1.15	1.13–1.17	4	0.77	0.75–0.80	2

For definition of solar distance, see Fig. 4E,F.

(Err_{med}) obtained with large and small apertures are compared (left *versus* right column). To avoid any possible influence of low polarization contrast (see above), only signal maxima with $d_{eff} \geqslant 0.10$ are considered. As expected, with cloudless skies (sky 0), both the general shape of the response curves (not shown) and the directional performance (Fig. 6A,B) were

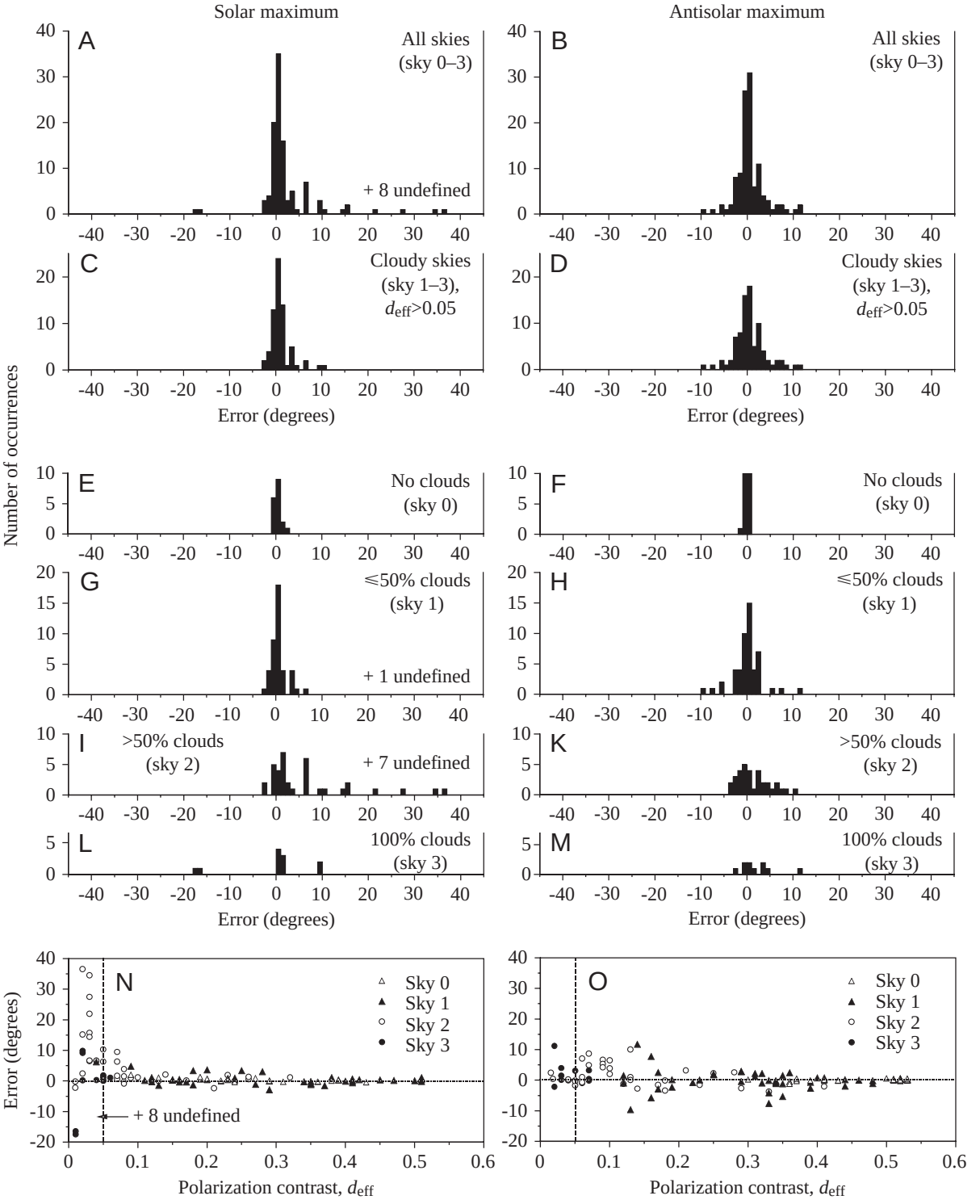

Fig. 5. Errors of the maxima of the polarization response curves (azimuth errors Err_{med}) in indicating the solar and the antisolar azimuth (left and right column, respectively). (A,B) Histograms of data including all skies (sky 0 to sky 3), (C,D) data for physiologically relevant polarization contrasts (d_{eff}>0.05) with cloudy skies (sky 1 to sky 3), (E–M) data plotted separately for different sky conditions (sky 0, 1, 2 or 3). (N,O) Azimuth errors as a function of polarization contrast d_{eff}. Different symbols code for sky conditions 0–3. Values of *N* are 115 (A, B, N and O), 70 (C) and 85 (D). Note that the errors are small with physiologically relevant stimuli (see C and D).

independent of visual field size (P=0.08). However, under cloudy skies (sky 1 to sky 3), the errors were significantly larger with the small apertures (Fig. 6 C,D; P<0.0001). Often, the response curves had irregular shapes and the maxima were asymmetric (Fig. 3C). This asymmetry is reflected in the relatively large differences of up to 4 ° between the azimuths of the maxima determined using the 'median method' (Az_{med}) and those obtained using the 'maximum-value method' (Az_{max}) under cloudy skies (Fig. 6H). For the 60 ° visual fields, these differences are much smaller (<1 °; Fig. 6G; P<0.0001), indicating quite symmetrical shapes of the maxima. These data support the hypothesis that the large visual fields of POL-neurones increase the stability of the polarization signal.

Discussion

The present field measurements with the opto-electronic model POL-neurone complement our previous electrophysiological laboratory experiments using real POL-neurones. Whereas the reliability of cricket POL-neurones was previously tested using noise-free polarized stimuli of various degrees of polarization (Labhart, 1996), the reliability of the natural polarization signal was assessed in the present study using a practically noise-free technical substitute for a POL-neurone.

The model POL-neurone implements the basic properties of cricket POL-neurones such as the size and position of the receptive field, the spectral sensitivity and the opponent mechanism. There are, however, some differences in detail. (1) Cricket POL-neurones receive input from a large number of ommatidia (Helbling and Labhart, 1997; T. Labhart, unpublished observations), whereas the model neurone uses just one pair of polarization-sensitive photoreceptors representing a macro-ommatidium. This simplification is justified because the e-vector tuning directions were found to be virtually invariant within the visual field of cricket POL-neurones (Labhart and Petzold, 1993; Petzold, 1999). (2) The polarization sensitivity of photoreceptors in the POL area of the cricket is approximately 10 (M. Blum and T. Labhart, in preparation). The polarization sensitivity of the model is given by the dichroic ratio of the polarizers, which is several thousand, i.e. virtually infinite for practical purposes. However, the exact polarization sensitivity of the system is irrelevant because the model response is not in neuronal units (e.g. spike frequency) but rather represents the celestial polarization stimulus as seen through the spatial, spectral and polarization-

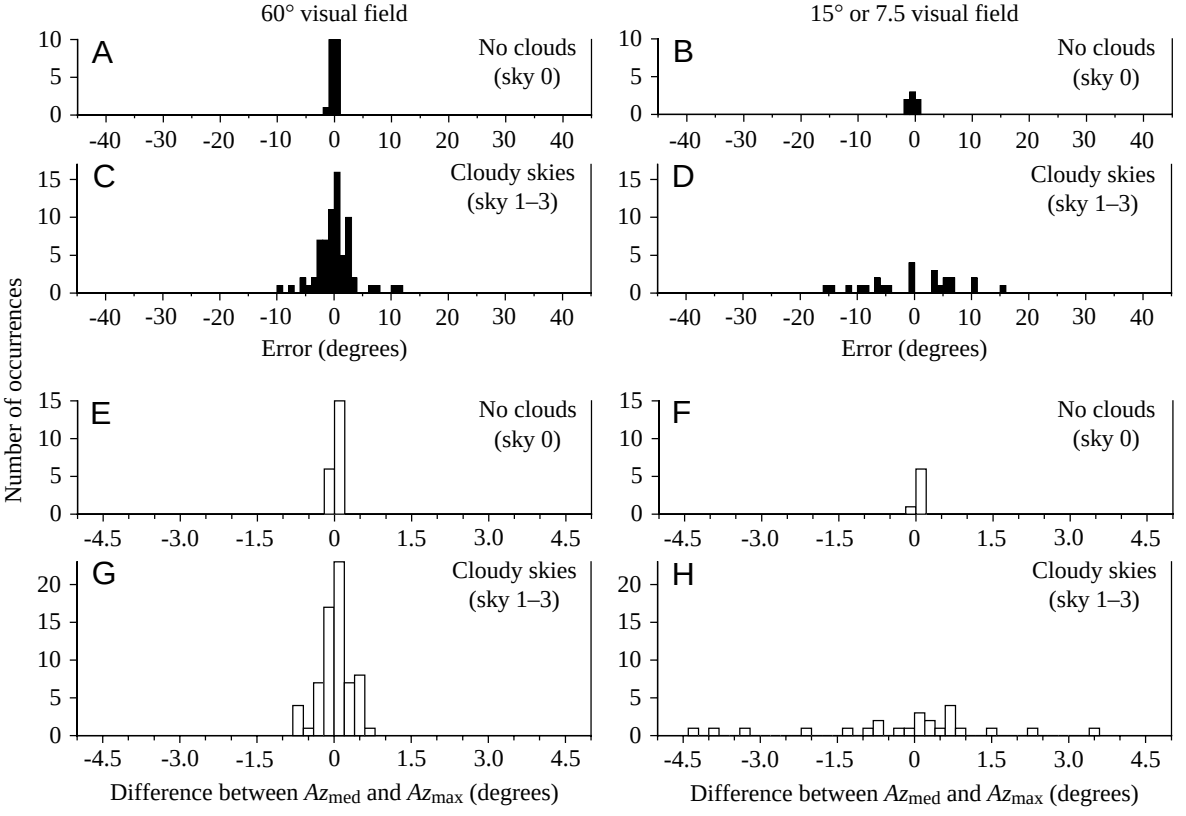

Fig. 6. Performance of the POL-neurone model with large (60 °) and small (15 ° or 7.5 °) visual fields (left and right column, respectively). Antisolar data with polarization contrast $d_{eff} \geqslant 0.10$ are presented. (A–D) Histograms of azimuth errors Err_{med} for cloudless skies (sky 0) (A,B) and cloudy skies (sky 1 to sky 3) (C,D). (E–H) Histograms for the differences between the azimuths indicated by the median method (Az_{med}) and those obtained using the maximum-value method (Az_{max}) (for definitions of Az_{med} and Az_{max}, see Materials and methods). (E,F) Cloudless skies (sky 0), (G,H) cloudy skies (sky 1 to sky 3). Values of N are 21 (A,E), 7 (B,F), 69 (C,G) and 24 (D,H). Note the inferior directional performance (compare D with C) and asymmetric maxima (compare H with G) with the small visual fields under cloudy conditions.

opponent filters of a POL-neurone (see below for the relationship between model and cricket POL-neurone response). The model neurone can also be regarded as a specialized measuring instrument for skylight polarization for which the highest possible polarization sensitivity is desirable. (3) In the cricket optic lobe, there are three types of POL-neurone tuned to different e-vector orientations, i.e. 10°, 60° and 130° with respect to the horizontal (Labhart and Petzold, 1993; Petzold, 1999), whereas our sole model POL-neurone was tuned to horizontal e-vectors. This study was not aimed at recording the responses of the exact tuning types of POL-neurones; instead, it was designed to assess the strength and quality of the celestial polarization signal available to cricket POL-neurones in general. The horizontal tuning orientation has the advantage that, for cloudless skies, the azimuths of the response maxima are precisely and easily predictable (solar and antisolar azimuth) and are independent of solar elevation (see Fig. 1B). In principle, the position of the maxima could also be predicted for other tuning angles if the polarization pattern behaved exactly according to Rayleigh rules (Strutt, 1871). In reality, both absolute values and gradients of radiance I and degree of polarization d in the sky are extremely variable and only poorly match theoretical predictions even in cloudless skies (Brines and Gould, 1982). Because of the gradient of e-vector orientation within the large visual field of the neurones, the gradients of I and d within the visual field will significantly influence the response, but to an unpredicable degree, and the prediction of the response maxima will, therefore, always be imprecise. However, for horizontal e-vectors, i.e. along the symmetry line of the polarization pattern (see Fig. 1B), the unpredictable influences of I and d on both sides of the symmetry line cancel each other out so that, for cloudless skies, there is no reason to expect deviations of the maxima from the predicted solar and antisolar azimuths. The cloudless sky thus provided a welcome control situation for assessing the overall precision of the measuring system.

The visual field of POL-neurones has been determined electrophysiologically by Petzold (1999). The border of the visual field is not sharp; instead, sensitivity tapers off at the rim. For the model, we chose an aperture of 60°, approximately corresponding to that part of the visual field of the neurone that is defined by at least 25% sensitivity, thus disregarding the outer, low-sensitivity range of the visual field. Because of the wider area of optical integration, including this outer range would slightly decrease the strength of the polarization signal (see Table 1), but would increase the precision of the signal under cloudy skies (see Fig. 6). Computer simulations of POL-neurones have shown that weighting the contributions of the different parts of the visual field according to relative sensitivity has a negligible influence on the response, at least within the high-sensitivity part of the visual field (Petzold, 1999). The flat sensitivity profile of the opto-electronic model neurone is, therefore, justified.

Strength of the polarization signal

In the present experiments, the polarization contrast d_{eff} did not exceed 0.53 even under optimal conditions. How does this value compare with previously published reports of skylight polarization? According to Rayleigh theory, the maximal degree of polarization d at 90° to the sun is approximately 0.85 in the blue, whereas measured values obtained in small patches of sky under optimal conditions (clear, dry sky at high altitude) reached approximately 0.75 (Coulson, 1988, p. 199ff, p. 275ff). Does the difference between the present and published maxima of polarization reflect a generally low skylight polarization in the Zurich area? First of all, the polarization contrast d_{eff} is not directly comparable with the conventional degree of polarization d, although it is defined in an analogous way (see Materials and methods). Remember that d_{eff} was obtained by scanning the upper part of the sky with an eccentric visual field, i.e. the observed part of the sky changed constantly as the model changed its azimuthal orientation. In contrast, the conventional degree of polarization d is defined as polarization contrast within a given (usually small) area of the sky. Fortunately, average degrees of polarization within the 60° visual field (d_{loc}, see Materials and methods) used in the present experiments can be determined from the data for the solar and antisolar azimuths, where the horizontal channel is exactly aligned with, and the vertical polarization channel is perpendicular to, the e-vector in the sky. The largest value of d_{loc} was 0.58. If this value is corrected for the large visual field using the factor 1.12 (calculated in the same way as the factor obtained for d_{eff} in the antisolar part of the sky, compare Table 1), 0.65 is obtained, which seems reasonable considering the relatively low altitude of Zurich (500 m) and indicates quite normal skylight polarization.

Our d values are also comparable with data from a recent video-polarimetric study of the sky. Average d values within a 40°×50° window in the zenith reached 0.58 at sunset but, interestingly, in individual pixels d was as high as approximately 0.7 (Horváth and Wehner, 1999). In another study, a mobile robot was equipped with polarization sensors based on the same principle as the POL-neurone model. The evaluation of the polarization signals, recorded during the navigation experiments with the robot, indicated that d within the zenithal 57° visual field never exceeded 0.51 (Lambrinos et al., 1997). Although both these studies were carried out under the clear, dry sky of the North African desert, the maximal values of d are in reasonable agreement with those obtained in Zurich.

Apparently, the contrast of the polarization signal that is available to a navigating insect is usually quite low. d_{eff} hardly exceeds 0.5, with the median value of d_{eff} in our (somewhat biased) sample being 0.13 in the solar half of the sky and 0.28 in the antisolar half of the sky. Factors degrading the amplitude of the polarization signal are (1) scattering effects of non-gaseous particles in the atmosphere, such as aerosols, dust, haze and, of course, clouds, and (2) high solar elevations, i.e. small solar distances. (3) Optical integration over a large area of the sky also plays a significant role, as indicated by the experiments with differently sized visual fields and by the video-polarimetric data mentioned above (Horváth and Wehner, 1999).

The present data can also be compared with those of a previous electrophysiological study, in which cricket POL-neurones were stimulated with polarized light of different degrees of polarization *d* (Labhart, 1996). In these experiments, the e-vector rotated continuously and spike frequencies were recorded as a function of e-vector orientation. The minimal *d* for signalling e-vector information turned out to be approximately 0.05. Thus, the polarization contrasts d_{eff} of celestial e-vector signals, which can be exploited by crickets under natural conditions, range from 0.53 (the maximum contrast observed in the present study) to 0.05 (the signalling threshold of cricket POL-neurones; Labhart, 1996). Representative examples of e-vector response curves for high (*d*=0.49), medium (*d*=0.19) and near-threshold (*d*=0.07) polarization are given in Labhart (1996, Fig. 3B–D). Of course, because the degree of polarization *d* remained constant during e-vector rotation, these curves show no differences between 'solar' and 'antisolar' maxima. Activity levels differed somewhat between individual POL-neurones. With a *d* of 0.5, spike activity oscillated between a maximum of 60–100 s^{-1} and a minimum of 0–4 s^{-1} (unpublished raw data from Labhart, 1996). At this comparatively high degree of polarization, the modulation of spike frequency often deviates from a sinusoidal shape, having flattened minima suggestive of clipping (see Labhart, 1996). With a *d* of 0.05, spike activity typically oscillated between approximately 30 s^{-1} and approximately 10 s^{-1}. Although these response curves are quite noisy, they still carry useful directional information (see Labhart, 1996).

As demonstrated above, cricket POL-neurones are perfectly able to handle the usually weak polarization signals present in the sky. No doubt the intrinsic polarization antagonism of POL-neurones plays a significant role in this high e-vector sensitivity by effectively enhancing the strength of skylight polarization. Apart from calculating the polarization contrast in the sky to which the POL-neurone model was exposed (optical d_{eff}, see Fig. 4A,B), the polarization contrast that the model experienced internally after the polarization-opponent filter has also been calculated (neuronal d_{eff}, see Fig. 4C,D). The median polarization contrasts rise from 0.13 and 0.28 (optical d_{eff}) to 0.26 and 0.52 (neuronal d_{eff}) for the solar and the antisolar half of the sky, respectively. Thus, many weak polarization signals, which would remain undetected by a single channel analyzer, may cross the detection threshold owing to the antagonism.

Directional information in the polarization signal

The celestial polarization signal as experienced by cricket POL-neurones is astonishingly robust. Directional information as indicated by the maximum of the POL-neurone model response is highly reliable even under cloudy conditions given enough polarization contrast (d_{eff}>0.05). In the sample taken under cloudy skies (Fig. 5C,D), the standard deviation of the azimuth error was only ±2.3° for the solar sky and ±3.4° for the antisolar sky (or ±2.6% and ±3.8% relative to the 180° period of a polarized stimulus). Previous electrophysiological experiments have shown that cricket POL-neurones indicate the e-vector with a reliability of approximately ±3° (standard deviation) with degrees of polarization *d* exceeding 0.1, and approximately ±6° for values of *d* between 0.05 and 0.1 (Labhart, 1996). Combining both stimulus and neuronal scatter gives total errors of approximately ±4° for medium *d* values and ±6.5° for low *d* values. Another characteristic trait of the model response curves is their smooth shape with symmetrical maxima (see Figs 1C, 3A,B), which may be important for further processing of the responses of the POL-neurone.

What factors stabilize the polarization signal? Both neuronal design and the properties of the celestial polarization pattern seem to contribute. (1) The POL-neurones filter out unstable and irrelevant features from the celestial stimulus: the polarization-antagonism makes the system insensitive to light intensity, the large visual field acts as a low-pass filter that serves to iron out local disturbances in the e-vector pattern, and monochromacy avoids interference with spectral gradients of skylight. Note, however, that the influence of the strength of the polarization signal, which affects the amplitude of the e-vector response curve, is not removed by the POL-neurones (see below). (2) The distribution of the degree of polarization *d* in the sky is strongly variable and rarely approaches the smooth gradient predicted by theory. However, skylight polarization is often present under seemingly unfavourable conditions, and the e-vector distribution is surprisingly stable. Although light reflected from clouds is principally unpolarized because of multiple scattering, clouds often appear polarized because of sunlight scattered in the column of air between the cloud and the observer (Brines and Gould, 1982; Können, 1985, p. 31; T. Labhart, unpublished observations). This is especially true for light and scattered clouds and can easily be observed by eye with the help of a sheet polarizer, or even better with a polarization axis finder (Edmund Scientific Company), and is most clearly seen at approximately 90° from the sun. Although the degree of polarization *d* seen against a cloud is considerably weaker than in adjacent areas of blue sky, the orientation of the e-vector is as expected for the unobstructed sky. e-vector information is, therefore, not necessarily abolished by clouds. However, because of the relatively weak or absent polarization of clouds, strongly asymmetric clouding can induce considerable azimuth errors in spite of the spatial low-pass filter. Note that, under total, thick overcast, the sky is unpolarized (Brines and Gould, 1982; present study). (3) In addition to neuronal filtering and relatively stable stimulus conditions, there is a geometrical factor stabilizing the neural response function. As the optical axis of the POL-neurone model deviates from the symmetry line of the polarization pattern, the mismatch between celestial e-vector and horizontal tuning direction of the model increases, which reduces the response level (see Fig. 3A). Thus, relatively weak but optimally oriented polarization along the symmetry line of the polarization pattern (for instance, with clouds) may elicit a stronger response than the high polarization of blue sky elsewhere. This effect automatically pushes the response maximum towards the solar or the antisolar azimuth.

Although POL-neurones contain efficient filters against the influences of light intensity, spectral gradients and irregularities of the polarization pattern, they are not insensitive to variations in the strength of the polarization signal. One consequence of this dependence is that solar elevation strongly influences the shapes of the POL-neurone response curves, i.e. the higher the sun, the greater the difference between the solar and the antisolar maximum (see Fig. 3A,B). This is because the visual field of POL-neurones is not directed to the zenith but approximately 25° away from it. In a zenith-centred system, the response curves would always be sinusoidal, i.e. both maxima would have the same amplitude, irrespective of solar elevation (see Fig. 1B). It is not unreasonable to assume that the processing of POL-neurone signals for extracting directional information is easier when the shapes of the response curves remain constant during the day. Thus, POL-neurones seem not to be optimally designed in this respect. Interestingly, each of the three tuning types of class 1 POL-neurone (Petzold, 1999) obtaining input from one eye has a corresponding type with a similar tuning direction obtaining input from the other eye (Labhart and Petzold, 1993; Petzold, 1999). Assuming that the signals of corresponding tuning types are pooled by more central neurones, these pooling neurones will combine two eccentric visual fields directed to opposite sides of the head, i.e. to the left and to the right (Petzold, 1999), thus implementing zenith-centred systems. Their response curves should, therefore, be sinusoidal with all solar elevations. Apart from this time-of-day independence, pooling may help to improve signal quality because two samples from largely different areas of the sky are combined.

We have tested these ideas by pooling signals obtained under quite noisy polarization conditions, i.e. by considering response curves in which the azimuth error was $\geqslant 5°$ or undefined in at least one of the maxima. The pooling procedure was as follows: a copy of the original response curve was phase-shifted by 180° (Fig. 7A), and the original and the shifted curve were added to each other. As the example in Fig. 7B demonstrates, the pooled response functions did, indeed, become sinusoidal. Large errors and undefined situations at the solar maximum (Fig. 7C) were absorbed by the antisolar maximum (Fig. 7E). The errors (Err_{med}) in the antisolar and the pooled maxima are statistically indistiguishable (compare Fig. 7D with Fig. 7E; P=0.42). Regarding the individual response curves, pooling brought both some gain (positive values in Fig. 7F) and some loss (negative values in Fig. 7F) of precision with respect to the original antisolar maximum. Overall, pooling had little influence on directional performance in the antisolar part of the sky but effectively absorbed useless and potentionally misleading information from the solar part of the sky.

Apart from demonstrating its potential usefulness, we have so far presented no evidence for bilateral pooling in the e-vector-detecting system of the cricket. The mere presence of corresponding tuning types of POL-neurones may be regarded as some circumstantial evidence. The finding that the axons of class 1 POL-neurones run all the way from one optic lobe to the other (Labhart and Petzold, 1993; Petzold, 1999) indicates that some cooperation between the two sides exists. Direct evidence for bilateral pooling was recently reported in an electrophysiological study on another orthopteran insect, the locust *Schistocerca gregaria*. The polarization-opponent TL2 neurones in the central complex of the brain were found to receive input from both eyes, and both inputs were tuned to the same e-vector (Vitzthum, 1997).

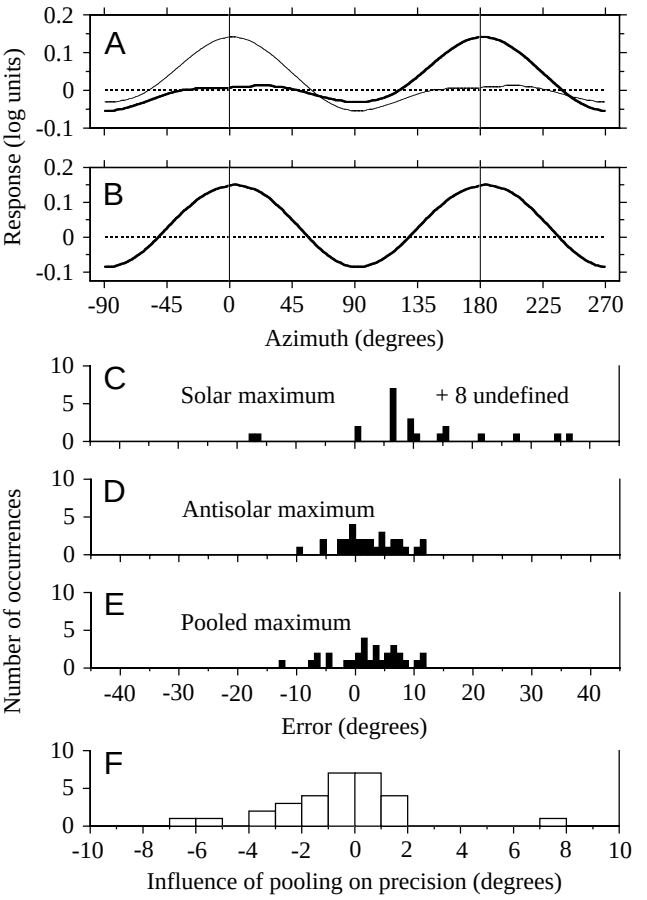

Fig. 7. Bilateral pooling of the signals of corresponding POL-neurones. (A,B) Pooling procedure: a copy of the original response curve (thick line in A) is phase-shifted by 180° (thin line), and the curves are added to each other (B). (C–F) The effect of pooling on performance. Only those response curves in which the azimuth errors (Err_{med}) of one or both maxima is greater than 5° or undefined are used. Histograms of Err_{med} for the solar (C), the antisolar (D) and the pooled (E) response. (F) Gain and loss in precision (positive and negative values, respectively) obtained by pooling with respect to the antisolar maximum; N=30. Note that pooling enhances performance by removing large errors and undefined situations at the solar maximum.

Although the shape of bilaterally pooled POL-neurone responses is largely independent of solar elevation and cloud conditions, the amplitude of the response remains a function of the strength of the polarization signal: the stronger the degree of polarization d in a given area of the sky (i.e. with a given e-vector), the stronger the (excitatory or inhibitory) response of the POL-neurone to that stimulus. However, as

demonstrated in honeybees, insects do not rely on the degree of polarization for navigation (Rossel and Wehner, 1984; Brines and Gould, 1979). This makes sense since both absolute values and gradient of polarization in the sky are very unreliable indicators of direction, whereas the e-vector pattern is quite stable (Brines and Gould, 1982, and see above). How does the nervous system deal with the variation in response amplitude or, in other words, how is the unused information about the degree of polarization removed from the system at a later stage of processing? Models of mechanisms for extracting directional information from POL-neurone signals have to take this into account.

The maximum azimuth error observed under physiologically relevant conditions was 12°. This indicates that navigation errors may be considerable under unfavourable circumstances. However, the temporal dimension has so far been disregarded. Even a strongly asymmetrical e-vector pattern may serve as a compass reference provided that the distortion remains more or less constant during a navigation period, for instance during a foraging excursion or while communicating a food source to bee recruits (Kirschfeld, 1988). Navigation experiments with *Cataglyphis fortis* indicate that this possibility can indeed be exploited by insects (Wehner, 1991). Although the experiments described in this study were not specifically designed for that purpose, the data contain a few time series demonstrating the temporal progression of the azimuth error under cloudy skies. As shown in Fig. 8, the azimuth errors remain quite stable over many minutes in most cases. In one case, the error of the solar maximum changed quite fast (Fig. 8A, uppermost curve). It turned out that bilateral pooling would effectively have buffered this rapid change, the pooled error values being −1.8°, 0° and −2.9°. For comparison, recruitment in bees takes just a few minutes (von Frisch, 1923). The duration of foraging excursions is, of course, dependent on the distance and nature of the food source. Honeybees complete visits to sugar-water feeders at up to a few hundred metres away within a few minutes, whereas excursions to scarcer and more distant food sources take much longer. Bees have been observed to forage several kilometres away from the hive (von Frisch, 1965, p. 67). Assuming a distance of 4 km and a flight speed of $8\,m\,s^{-1}$ (von Frisch, 1965, p. 195), the round trip, excluding time for nectar collection, takes 17 min. Clearly, under adverse sky conditions, navigating insects must also rely on non-celestial orientation cues such as landmarks, even for long-distance travel (e.g. Dyer, 1996).

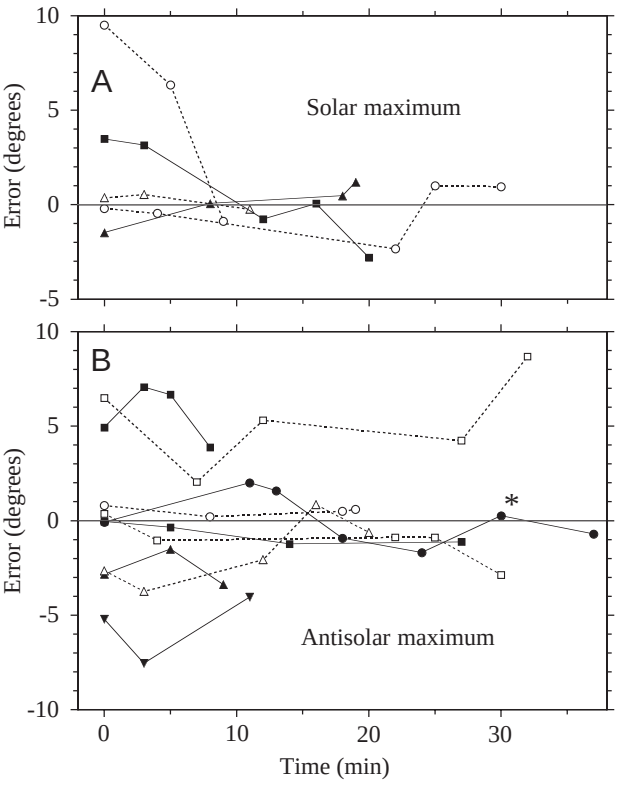

Fig. 8. Time course of azimuth errors Err_{med} with cloudy skies (sky 1 and sky 2) for the solar (A) and for the antisolar (B) maxima. Only time series with polarization contrasts $d_{eff} \geqslant 0.05$ are shown (except for one case where $d_{eff}=0.04$, marked by an asterisk in B). Note that the azimuth errors remain quite stable over many minutes in most cases.

Conclusions

In conclusion, the experiments reported here show that the polarization signal of the sky as experienced by a POL-neurone is very robust, indicating that the insect polarization compass is reliable even under cloudy weather conditions. This is due both to the relative stability of the e-vector pattern and to the filtering properties of the neurone. (1) The intrinsic polarization-antagonism not only enhances e-vector contrast but also removes intensity information, i.e. the neurone acts as a differential polarization filter. This mechanism seems to be powerful enough to have evolved independently in several insect orders (Labhart and Meyer, 1997). Although in five insect orders evidence for polarization-opponency is based on the architecture of the dorsal rim ommatidia alone, there is direct electrophysiological evidence in orthopterans (*Gryllus campestris*, *Schistocerca gregaria*: e.g. Labhart, 1988; Vitzthum, 1997) and hymenopterans (*Cataglyphis bicolor*: T. Labhart, unpublished observations). (2) The large visual field acts as a spatial low-pass filter that serves to even out local disturbances in skylight polarization. In crickets, this filter is based both on optical integration by the greatly enlarged visual fields of the dorsal rim photoreceptors (Labhart et al., 1984) and on neural integration by the POL-neurones, which obtain input from a large number of dorsal rim ommatidia (Helbling and Labhart, 1997; T. Labhart, unpublished observations). Structural modifications causing extended visual fields in dorsal rim ommatidia have also been reported in many other insect species of different orders (for a review, see Labhart et al., 1992; Meyer and Labhart, 1993), and in *Cataglyphis* there is electrophysiological evidence for neural integration (T. Labhart, unpublished observations). Although enlarging the visual field reduces the strength of the polarization signal (see Table 1), it strongly increases signal quality when the polarization pattern is disturbed by clouds (compare Fig. 3B

with Fig. 3C, and Fig. 6C with Fig. 6D). (3) Monochromacy, which implies colour blindness, avoids interference between spectral and e-vector information in a manner similar to that occurring in motion detection (Srinivasan, 1985).

This work was supported by the Swiss National Science Foundation grant 31.43317.95. I thank Hansruedi Helbling, Dan-Eric Nilsson, Jürgen Petzold and Rüdiger Wehner for critical comments on the manuscript.

References

Brines, M. L. and Gould, J. L. (1979). Bees have rules. *Nature* **206**, 571–573.

Brines, M. L. and Gould, J. L. (1982). Skylight polarization patterns and animal orientation. *J. Exp. Biol.* **96**, 69–91.

Brunner, D. and Labhart, T. (1987). Behavioural evidence for polarization vision in crickets. *Physiol. Ent.* **12**, 1–10.

Burghause, F. M. H. R. (1979). Die strukturelle Spezialisierung des dorsalen Augenteils der Grillen (Orthoptera, Grylloidea). *Zool. Jb. Physiol.* **83**, 502–525.

Coulson, K. L. (1988). *Polarization and Intensity of Light in the Atmosphere*. Hampton: A. Deepak Publishing.

Dyer, F. C. (1996). Spatial memory and navigation by honeybees on the scale of the foraging range. *J. Exp. Biol.* **199**, 147–154.

Helbling, H. and Labhart, T. (1997). Ommatidial arrangement and e-vector tuning in polarization-sensitive interneurons of crickets. *Proceedings of the 25th Göttingen Neurobiology Conference* (ed. N. Elsner and H. Wässle), p. 475. Stuttgart, New York: Thieme Verlag.

Herzmann, D. and Labhart, T. (1989). Spectral sensitivity and absolute threshold of polarization vision in crickets: a behavioral study. *J. Comp. Physiol.* A **165**, 315–319.

Homberg, U. and Würden, S. (1997). Movement-sensitive, polarization-sensitive and light-sensitive neurons of the medulla and accessory medulla of the locust, *Schistocerca gregaria*. *J. Comp. Neurol.* **386**, 329–341.

Horváth, G. and Wehner, R. (1999). Skylight polarization as perceived by desert ants and measured by video polarimetry. *J. Comp. Physiol.* A (in press).

Kirschfeld, K. (1988). Navigation and compass orientation by insects according to the polarization pattern of the sky. *Z. Naturforsch.* **43c**, 467–469.

Können, G. P. (1985). *Polarized Light in Nature*. Cambridge: Cambridge University Press.

Labhart, T. (1988). Polarization-opponent interneurons in the insect visual system. *Nature* **331**, 435–437.

Labhart, T. (1996). How polarization-sensitive interneurones of crickets perform at low degrees of polarization. *J. Exp. Biol.* **199**, 1467–1475.

Labhart, T., Hodel, B. and Valenzuela, I. (1984). The physiology of the cricket's compound eye with particular reference to the anatomically specialized dorsal rim area. *J. Comp. Physiol.* A **155**, 289–296.

Labhart, T. and Meyer, E. P. (1997). POL areas of compound eyes: the specialized e-vector detecting organs of insects. In *Proceedings of the 25th Göttingen Neurobiology Conference* (ed. N. Elsner and H. Wässle), p. 449. Stuttgart, New York: Thieme Verlag.

Labhart, T., Meyer, E. P. and Schenker, L. (1992). Specialized ommatidia for polarization vision in the compound eye of cockchafers, *Melolontha melolontha* (Coleoptera, Scarabaeidae). *Cell Tissue Res.* **268**, 419–429.

Labhart, T. and Petzold, J. (1993). Processing of polarized light information in the visual system of crickets. In *Sensory Systems of Arthropods* (ed. K. Wiese, F. G. Gribakin, A. V. Popov and G. Renninger), pp. 158–168. Basel, Boston, Berlin: Birkhäuser Verlag.

Lambrinos, D., Maris, M., Kobayashi, H., Labhart, T., Pfeifer, R. and Wehner, R. (1997). An autonomous agent navigating with a polarized light compass. *Adaptive Behav.* **6**, 131–161.

Laughlin, S. B. (1981). Neural principles in the peripheral visual systems of invertebrates. In *Comparative Physiology and Evolution of Vision in Invertebrates B, Invertebrate Visual Centers and Behavior I* (ed. H. Autrum), pp. 133–280. Berlin, Heidelberg, New York: Springer-Verlag.

Meyer, E. P. and Labhart, T. (1993). Morphological specializations of dorsal rim ommatidia in the compound eye of dragonflies and damselflies (Odonata). *Cell Tissue Res.* **272**, 17–22.

Müller, M. (1997). Anatomische und funktionelle Charakterisierung der unteren Einheit des Zentralkörpers im Gehirn der Heuschrecke *Schistocerca gregaria*. PhD thesis, University of Regensburg.

Müller, M. And Homberg, U. (1994). Influence of visual stimuli on the activity of neurons in the central complex of the locust *Schistocerca gregaria*. In *Proceedings of the 22nd Göttingen Neurobiology Conference* (ed. N. Elsner and H. Breer), p. 462. Stuttgart, New York: Thieme Verlag.

Nilsson, D. E., Labhart, T. and Meyer, E. P. (1987). Photoreceptor design and optical properties affecting polarization sensitivity in ants and crickets. *J. Comp. Physiol.* A **161**, 645–658.

Petzold, J. (1999). Polarisationsempfindliche Neuronen im Sehsystem der Feldgrille, *Gryllus campestris*: Elektrophysiologie, Anatomie und Modellrechnungen. PhD thesis, University of Zürich (in press).

Petzold, J. and Labhart, T. (1993). Polarization-opponent interneurons of crickets: absolute threshold, visual field properties and response to low degrees of polarization. In *Proceedings of the 21st Göttingen Neurobiology Conference* (ed. N. Elsner and M. Heisenberg), p. 371. Stuttgart, New York: Thieme Verlag.

Rossel, S. and Wehner, R. (1984). How bees analyse the polarization patterns in the sky. *J. Comp. Physiol.* A **154**, 607–615.

Schwind, R. and Horváth, G. (1993). Reflection-polarization patterns at water surfaces and correction of a common representation of the polarization pattern of the sky. *Naturwissenschaften* **80**, 82–83.

Srinivasan, M. V. (1985). Shouldn't directional movement detection necessarily be 'colour-blind'? *Vision Res.* **25**, 997–1000.

Strutt, J. (Lord Rayleigh) (1871). On the light from the sky, its polarization and colour. *Phil. Mag.* **41**, 107–120.

Vitzthum, H. (1997). Der Zentralkomplex der Heuschrecke *Schistocerca gregaria*: Ein mögliches Zentrum des Polarisationssehens. PhD thesis, University of Regensburg.

Vitzthum, H., Müller, M. and Homberg, U. (1997). Polarization-sensitive interneurons in the central complex of the locust *Schistocerca gregaria*. In *Proceedings of the 25th Göttingen Neurobiology Conference* (ed. N. Elsner and H. Wässle), p. 470. Stuttgart, New York: Thieme Verlag.

von Frisch, K. (1923). Ueber die 'Sprache' der Bienen, eine tierphysiologische Untersuchung. *Zool. Jb. Physiol.* **40**, 1–186.

von Frisch, K. (1965). *Tanzsprache und Orientierung der Bienen*. Berlin, Heidelberg, New York: Springer.

Wehner, R. (1991). Visuelle Navigation: Kleinsthirn-Strategien. *Verh. Dt. Zool. Ges.* **84**, 89–104.

Zufall, F., Schmitt, M. and Menzel, R. (1989). Spectral and polarized light sensitivity of photoreceptors in the compound eye of the cricket (*Gryllus bimaculatus*). *J. Comp. Physiol.* A **164**, 597–608.